JOURNAL OF FORENSIC SCIENCES

J Forensic Sci, November 2012, Vol. 57, No. 6
doi: 10.1111/j.1556-4029.2012.02181.x
Available online at: onlinelibrary.wiley.com

PAPER

ANTHROPOLOGY

Pierre Guyomarc'h,[1,2] *Ph.D. and Carl N. Stephan,*[2,3] *Ph.D.*

The Validity of Ear Prediction Guidelines Used in Facial Approximation*,†,‡

ABSTRACT: This study examined eight previously published ear prediction methods by Welcker, Gerasimov, Fedosyutkin and Nainys, and Broadbent and Mathews. Computed tomography scans of 78 living adults (n_1) did not support any of these previously published recommendations. Free earlobes were found to accompany protruding supramastoid crests (Pearson's $\chi^2 < 0.05$); and ear length [l] and width [w] differed by sex ($p < 0.05$), correlated with age ($r = 0.38$[l]; 0.32[w]), and correlated with facial height ($r = 0.37$[l]; 0.30[w]). New regression equations (for ear length and width) were generated using these variables in several samples and, where possible, cross-validated using independent data ($n_1 = 78$, $n_2 = 2190$, $n_3 = 1328$, $n_4 = 1010$, and $n_5 = 47$). As a result of these analyses, four valid and tested methods for ear prediction were identified, but large degrees of error continue to make accurate prediction of the ear, from the skull, problematic.

KEYWORDS: forensic science, facial reconstruction, facial reproduction, external ear, pinna, skull

Facial approximation is used to estimate a face from a bare skull under blind conditions, that is, without *a priori* knowledge of the individual's facial appearance. Irrespective of the specific method used, the long-standing aim of facial approximation has been to produce a face, from the skull, that is correctly and easily recognized (1–9). Not only does this goal give facial approximation its greatest utility for the resolution of forensic cases, but as a duality it also necessitates the use of accurate soft-tissue prediction methods.

Over the last 10 years, tests have revealed that established face prediction methods perform suboptimally. This includes large inaccuracies for popular methods to determine mouth width (10,11), eyeball position (12–15), nose projection (16,17), and the *temporalis* muscle form (18). This has led to improved methods to determine these facial components (see the aforementioned studies and also [19–21]). However, the accuracy of preexisting and untested methods for other facial regions, including the ears, is unknown.

As part of the ongoing work to improve facial approximation methods, these other guidelines must be verified. Even if ears may contribute less to facial recognition than other facial components such as the eyes (22,23), evaluation of these prediction guidelines is important as auricles nevertheless are required for overall correct gestalt appearance of the face. Moreover, their importance is probably elevated for persons possessing more atypical features (e.g., large protruding ears). Although multiple ear prediction guidelines exist, few of these have been subject to empirical validation.

The assessment of the ear in relation to the skull, at least as it pertains to facial approximation and craniofacial superimposition work, was first undertaken by Welcker (24). Welcker (24) stated that the cartilaginous opening of the ear is placed more posterior and superior than the bony opening (mean displacement = 5.3 mm)—a guideline that has stood up to scrutiny (25). In addition, Welcker (24) was the first to state that the main axis of the ear is parallel to the ascending *ramus* of the mandible (Fig. 1*a*)—a guideline that has been extensively cited in the published facial approximation literature, but without empirical backing from experimental data (see, e.g., [5,9,26–28]).

In 1955, Gerasimov added that the ear length (=height) roughly approximates the height of the nose measured from the base to the glabella (Fig. 1*b*)—a recommendation based, in part, on data collected from 462 Tajiks by Ginzburg (9). In later years, Gerasimov modified this rule to the ear representing the height of the nose from glabella to subnasale, plus an additional 2 mm (29). By using the distance between nasion to nasospinale on the skull, Jordanov (28) suggests that Gerasimov's directions can be directly applied to skulls, and concludes from measurements of 161 Bulgarians that

[1]Université Bordeaux 1, UMR 5199 – PACEA, Anthropologie des Populations Passées et Présentes (A3P), Avenue des Facultés, Bâtiment B8, 33405 Talence Cedex, France.

[2]Joint POW/MIA Accounting Command, Central Identification Laboratory, 310 Worchester Avenue, Building 45, Hickam Air Force Base, HI 96853.

[3]Anatomy and Developmental Biology, School of Biomedical Sciences, The University of Queensland, Brisbane, 4072 Qld, Australia.

*Portions of this work have been presented at the 63rd Annual Meeting of the American Academy of Forensic Sciences, February 21–26, 2011, in Chicago, IL.

†Supported, in part, by an appointment to the Postgraduate Research Participation Program at the Joint POW/MIA Accounting Command-Central Identification Laboratory, administered by the Oak Ridge Institute for Science and Education through an interagency agreement between the U.S. Department of Energy and the JPAC-CIL. Financial support for this work has also been provided by a Ph.D. scholarship granted by the French Ministry of Research (*Ministère de l'Enseignement Supérieur et de la Recherche*), and by a BQR (*Bonus Qualité Recherche* "*Reconstitution faciale par imagerie 3D*") obtained by H. Coqueugniot.

‡The views and opinions contained herein are solely those of the authors and are not to be construed as official, or as views of the U.S. Department of Defense and/or any of the U.S. Armed Forces.

Received 16 May 2011; and in revised form 12 Sept. 2011; accepted 1 Oct. 2011.

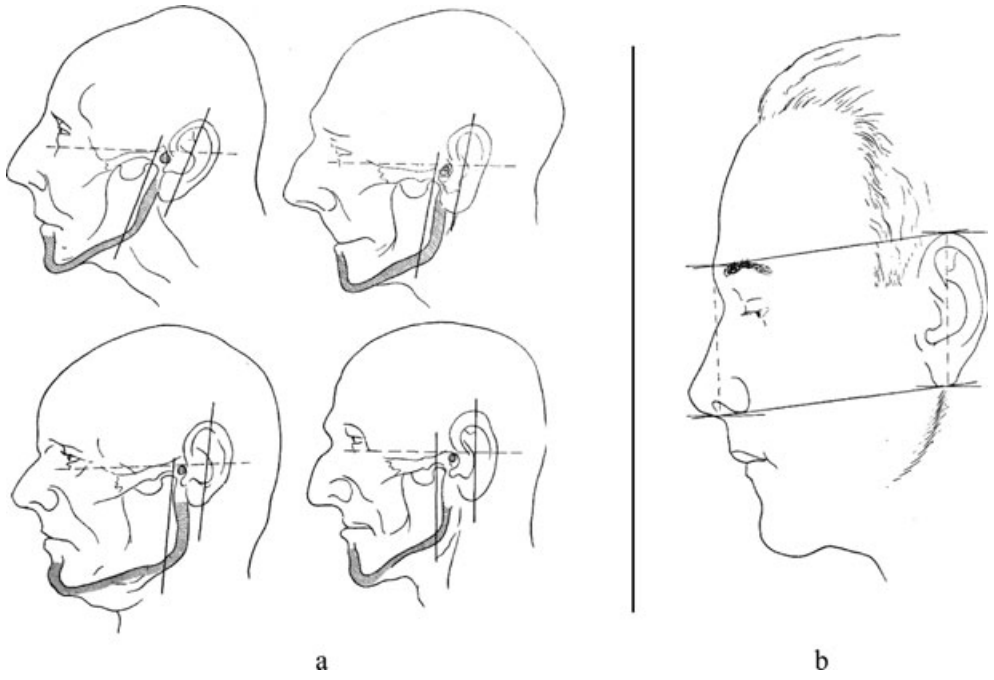

FIG. 1—*Illustrations depicting the proposed equality between the angle of the jaw line and the main axis of the ear (a), and between the height of the ear and the length of the nose (b). Figures extracted from Gerasimov (9).*

Gerasimov's rules are correct: that is, only slight differences existed between the "height of the nose" and the height of the ear (*c.* 2 mm).

Other practitioners have also suggested that the height of the nose equals the height of the ear without the glabella qualifier (30–32), implying that the height of the nose represents the distance from sellion to subnasale. This latter guideline cannot be valid, however, because 95% of people possess ears that are, on average, c.10 mm larger than their noses (33,34). Krogman and Iscan (31) have also stated that the ear's height should equal 50 mm; however, numerous metric studies contradict this suggestion, with mean ear height measurements in the vicinity of 60–70 mm (see, e.g., data summarized by Martin [35, p. 572], or Table 1 for more contemporary publications).

Other guidelines that Gerasimov (9) suggested, many of which have been restated by Fedosyutkin and Nainys (32) and Jordanov (28), include the following: (i) small and medially directed mastoid processes reflect small ears close to the head; (ii) massive and prominent mastoid processes denote a large and spread ears; (iii) a strongly developed supramastoid crest indicates a laterally projecting superior half of the ear; (iv) a rough external surface of the mastoid process indicates a laterally projecting inferior half of the ear; (v) a combination of the skeletal characteristics in "iv" and "v" gives a completely protruding ear (i.e., at both upper and lower poles); and (vi) the breadth of the ear equals half of its length. Note that this latter guideline appears to be inaccurate since typical ear index values reported in the early anthropological literature *c.* 0.60 (for summary, see Martin [35, p. 573]).

Broadbent and Mathews (27) in a review of artistic guidelines pertinent to surgical plastic facial reconstruction (that have been adopted for facial approximation) stated that the main axis of the ear was parallel to the angle of the dorsum of the soft tissue nose. This rule has since been invalidated by both Skiles and Randall (47) and Farkas et al. (33,34,48) who found that the ear inclination is as much as 15° more toward the vertical.

Fedosyutkin and Nainys (32) have also added that (i) the earlobe is free if the mastoid process is pointing forward (skull in Frankfurt Horizontal) and (ii) the earlobe is attached if the mastoid process points more inferiorly. These observations were reportedly based on more than 200 skulls of identified individuals for whom facial photographs existed; however, trait frequencies and actual measurements are not provided in the original article (32).

It is worth noting here that the early anthropometric literature identifies differences in ear measurements according to sex (males larger than females) and the size of earlobe between individuals (for summary, see Martin [35]). The common, but typically informal, observation that ear size increases with age, and is associated with body size, has also been subject to recent empirical studies (40,44,45); however, these investigations have typically gone unmentioned in the facial approximation literature. Regression equations for ear length prediction have also been reported (see Table 2), but are limited because their errors are rarely fully disclosed, cross-validation results have not been pursued, and the practical value of the regressions, as relevant to facial approximation, has not been considered.

Recently, two further regression equations have been proposed to predict ear dimensions for males and females based on skeletal facial height (see equations no. 5 and 6 in Table 2, after Balueva et al. [49]). However, indicators of the accuracy of these equations (e.g., confidence intervals, r^2, or standard errors of the estimate [SEE]) are not presented by the original authors (49). This makes it difficult to judge the value of the methods, especially because these equations were formulated on the basis of correlations to facial height measurements on living subjects, not facial heights on skulls as the regression equations require.

This article aims to clarify the validity of some of the abovementioned ear prediction methods and attempts improvements using recently acquired medical computed tomography (CT) scans of living adults. To provide comprehensive assessments, four other samples of ear data are also drawn upon for cross-validation tests of regression equations. These data sets include (i) 2190 three-dimensional (3D) facial scans of U.K. individuals by Evison and Vorder Bruegge (50); (ii) caliper measurements of 1328 White

TABLE 1—*Mean adult ear heights (mm) published in the literature. Where sides were not combined in the original study, the information for the left side has been reported.*

Mean	SD	Min	Max	*n*	Age (Years)	Sample	Study	Method
Females								
59.7	3.0	–	–	150	18–25	Turks	(37)	Sliding caliper
62.2	–	–	–	89	19–65	Rhode Island Hospital	(38)	Sliding caliper
59.9	3.5	–	–	200	19–25	U.S. Caucasoids	(34)	Sliding caliper
57.6	3.9	–	–	30	18	Chinese	(36)	Sliding caliper
57.4	3.5	–	–	73	18–30	White North Italians	(39)	3D digitizer
60.3	3.2	–	–	38	31–56	White North Italians	(39)	3D digitizer
58.5	3.9	47.0	70.0	108	Adults	Bulgarians	(28)	Not reported
64.0	5.4	47.0	82.0	*c.* 431	20–90	Dutch	(40)	Photogrammetry
56.4	4.1	–	–	66	18–30	White Italians	(41)	3D digitizer
61.6*	4.2*	–	–	64	31–80	White Italians	(41)	3D digitizer
Males								
67.1	4.5	53.8	79.7	500	22–34	USAF Flight Personnel	(42)	Photogrammetry
63.1	3.6	–	–	191	18–25	Turks	(37)	Sliding caliper
65.2	–	–	–	34	18–61	Rhode Island Hospital	(38)	Sliding caliper
57.7	–	–	–	121	18–30	Indian (South East Asian)	(43)	Sliding caliper
61.2†	–	–	–	294	30–70	Indian (South East Asian)	(43)	Sliding caliper
62.9	3.5	–	–	109	19–25	U.S. Caucasoids	(34)	Sliding caliper
60.7	3.8	–	–	30	18	Chinese	(36)	Sliding caliper
63.2	4.0	–	–	89	18–30	White North Italians	(39)	3D digitizer
65.3	4.1	–	–	41	31–56	White North Italians	(39)	3D digitizer
62.9	2.8	55.0	70.0	53	Adults	Bulgarians	(28)	Not reported
71.0	5.5	50.0	89.0	*c.* 911	20–90	Dutch	(40)	Photogrammetry
62.2	4.1	–	–	126	18–30	White Italians	(41)	3D digitizer
65.8*	4.7*	–	–	99	31–80	White Italians	(41)	3D digitizer
Both sexes								
67.5	–	52.0	84.0	206	30–93	Varied population groups	(44)	Not reported
70.1	–	50.0	87.0	400	21–94	Japanese	(45)	Not reported
66.6	4.5	55.0	83.0	815	Not reported	Fijians	(46)	Sliding caliper

*Weighted mean and standard deviation calculated by combining the original samples of 31–40, 41–50, 51–64, and 65–80 years.
†Weighted mean calculated by combining original samples of 30–40, 40–50, 50–60, and 60–70 years.

American cadavers by T. W. Todd (unpublished data, courtesy of the Cleveland Museum of Natural History); (iii) caliper measurements of 1010 Black American cadavers by T. W. Todd (unpublished data, courtesy of the Cleveland Museum of Natural History); and (iv) caliper measurements of 47 contemporary living subjects taken specifically for this study.

Material and Methods

CT scans of 78 living subjects (n_1), 43 males and 35 females, of known age (mean age = 41 years; SD = 19 years; range = 18–84 years) were used in this study so that soft tissue profiles of the ears, and their relationship to the skulls of the same individuals, could be examined. The scans represented medical images, collected from French Hospitals, with the subjects in the supine position and without any mechanical pressure on the ears. Patients presenting trauma or pathologies that affected the facial region were excluded. This sample, thereby, represents a much smaller component of a larger cohort, that is, CT scans of 500 individuals that were all screened for suitability to be used in this study. Ethical approval for the collection of the CT data was obtained from the French *Comité de protection des personnes* (*Sud-Ouest et Outre Mer III*). The slice thickness of scans in this sample was variable, but commonly <1 mm (range = 0.6–1.4 mm).

CT scans were viewed using the Treatment and Increased Vision for Medical Imaging (TIVMI) software developed by Bruno Dutailly (UMR 5199 PACEA). This software is freely downloadable (http://www.pacea.u-bordeaux1.fr/TIVMI/) and in addition to possessing classic geometric operators (such as planes, lines, segments, and outlines), it holds the advantage that 3D surface reconstruction can be undertaken using the Half-Maximum Height protocol (51). This allows for a more accurate detection of the interface between tissues such as bone and soft tissue in contrast to other methods such as Marching Cubes algorithm (52).

Once the osseous and cutaneous surfaces were rendered from the DICOM files in the TIVMI software, landmarks were established in 3D both on the soft tissues of the ear and on the skull (Tables 3 and 4, Figs 2–4). In addition, morphoscopic assessment of the size of the supramastoid crest (Fig. 5) was used to evaluate the covariation of this feature with lateral ear protrusion. The morphology of the earlobe (attached or free) was also morphoscopically determined (Fig. 6) to evaluate its covariation with the skull following the recommendations of Fedosyutkin and Nainys (32).

Table 5 and Figs 2–4 present the measurements (angles and linear distances) that were used to evaluate the following preestablished ear prediction rules:

(i) The main axis of the ear is parallel to the ascending *ramus* of the mandible (24), that is, EA compared to MRA.
(ii) The height of the ear approximates the height of the nose (9,30–32), that is, sa-sba compared to n-ss, g'-sn, se-sn, etc.
(iii) The height of the ear approximates the height of the nose from glabella to subnasale plus 2 mm (Gerasimov cited in [29]), that is, sa-sba compared to g-ss + 2 mm.
(iv) A small and medially directed mastoid process reflects small ears close to the head, and a massive and prominent mastoid process denotes a large and spread ear (9), that is, MLA and MDH compared to ELA, sa-sba, and pra-pa.
(v) The breadth of the ear equals half of its length (9), that is, pra-pa/sa-sba = 0.5.

TABLE 2—*Regression equations for ear prediction.*

Equation No.	Ear Dimension	Formulae	Sex	Population	*n*	r^2	SEE	Data
1	Length	(0.22 * age) + 55.9	Both	U.K.	206	UR	UR	(44)
2	Length	(0.13 * age) + 61.8	Both	Japan	400	0.09	UR	(45)
3	Length	(0.12 * stature) + 51.2	Both	Japan	400	0.04	UR	(45)
4	Length/Stature	(0.00019 * age) + 0.034	Both	Japan	400	0.36	UR	(45)
5	Length	55.488 + 0.073 * (FHN + 6)	Males	Russia	UR	UR	UR	(49)
6	Length	45.650 + 0.110 * (FHN + 6)	Females	Russia	UR	UR	UR	(49)
7	Length	(5.89 * sex) + (0.21 * age) + 52.36	Both	Mostly U.K.	2190	0.47	4.3	(50)
8	Length	(5.06 * sex) + (0.15 * age) + 55.90	Both	U.S. White	1328	0.21	5.4	Todd
9	Width	(3.04 * sex) + (0.05 * age) + 33.2	Both	U.S. White	1010	0.11	3.5	Todd
10	Length	(2.13 * sex) + (0.16 * age) + 54.20	Both	U.S. Black	1328	0.21	5.2	Todd
11	Width	(2.06 * sex) + (0.07 * age) + 32.9	Both	U.S. Black	1010	0.19	3.1	Todd
12	Length	(4.85 * sex) + (0.10 * age) + 54.95	Both	France	78	0.33	4.7	This study
13	Length	(sex–0.55)/0.5) + (age–41.4)/18.8)[†]	Both	France	78	0.33	6.9	This study
14	Width	(3.20 * sex) + (0.05 * age) + 33.02	Both	France	78	0.29	3.1	This study
15	Length	(3.98 * sex) + (0.12 * FHN) + 45.44	Both	France	62	0.22	5.1	This study
16	Length	(3.68 * sex) + (0.15 * age) + (0.14 * FHN) + 37.63	Both	France	62	0.45	4.4	This study
17	Width	(3.29 * sex) + (0.07 * age) + (0.06 * FHN) + 29.22	Both	France	62	0.36	3.0	This study
18	Length	(4.95 * sex) + (0.19 * age) + 53.05	Both	Mixed	4653	0.38	5.1	Combined CT and caliper data of this study, Todd, and Evison and Vorder Bruegge

FHN, facial height of the skull; age, chronological age in years; sex, dichotomous dummy variable (females = 0, and males = 1); CT, computed tomography; SEE, standard errors of the estimate; UR, unreported.

[†]To convert standardized predicted ear length to millimeter, employ the formula: Ear Length (mm) = (Standardized Predicted Ear Length * 5.64) + 61.94. This calculation and the unit-weighted regression are based on means and standard deviations observed in the CT scan sample (n_1).

TABLE 3—*Soft tissue landmarks used in this study. All landmarks are defined with the head in the Frankfurt Horizontal.*

Name	Abbreviation	Locality	Definition
Otobasion superius	obs	Bilateral	Point of attachment of the helix in the temporal region*
Otobasion inferius	obi	Bilateral	Point of attachment of the ear lobe to the cheek*
Superaurale	sa	Bilateral	Most superior point on the free margin of the auricle*
Subaurale	sba	Bilateral	Most inferior point on the free margin of the auricle*
Preaurale	pra	Bilateral	Most anterior point of the ear located just in front of the otobasion superius*
Postaurale	pa	Bilateral	Most posterior point on the free margin of the ear*
Helix laterale	hx	Bilateral	Most lateral point on the superior part of the helix of the ear
Sellion	se	Midline	Deepest landmark located on the bottom of the nasofrontal angle*
Pronasale	prn	Midline	Most anterior point of the apex nasi (tip of the nose)*
Subnasale	sn	Midline	Apex of the angle at the columella base where the lower border of the nasal septum and the surface of the upper lip meet*
Soft tissue glabella	g'	Midline	Soft tissue analog of hard tissue glabella*

*After (53).

(vi) A strongly developed supramastoid crest corresponds to an upper protrusion of the ear (9), that is, supramastoid crest protrusion compared to EP, EA, and EIA.

(vii) The earlobe is attached if the mastoid process is directed downward and free if the mastoid process points forward (32), that is, earlobe morphology (free or attached) compared to MAA.

(viii) The main axis of the ear is parallel to the angle of the bridge of the nose (27), that is, EA compared to NRA.

This study consequently evaluated a total of eight previously suggested (nonregression) guidelines, two of which have been examined on prior occasions but which were retested here for repeatability purposes (guidelines ii and viii; see [28,33,34,47]). The six other ear prediction guidelines have never been subject to published scientific review.

In order to explore the relationships between the mastoid, ear angles, nose angles, ear heights, and nose heights, a matrix correlation was undertaken in addition to the aforementioned tests.

TABLE 4—*Hard tissue landmarks used in this study. All landmarks are defined with the head in the Frankfurt Horizontal.*

Name	Abbreviation	Locality	Definition
Glabella	g	Midline	Most anterior point of the frontal bone, between the superciliary arches*
Nasion	n	Midline	Point located at the intersection of the nasofrontal suture*
Rhinion	rhi	Midline	Most anterior point of the internasalis suture*
Subspinale	ss	Midline	Apex of curve under the nasal spine*
Mastoidale	ms	Bilateral	Most inferior point of the mastoid process*
Antero-inferior mastoid	mai	Bilateral	Most antero-inferior point of the mastoid process
Menton (or gnathion)	gn	Midline	Lowest median landmark on the lower border of the mandible†

*After (54).
†After (55).

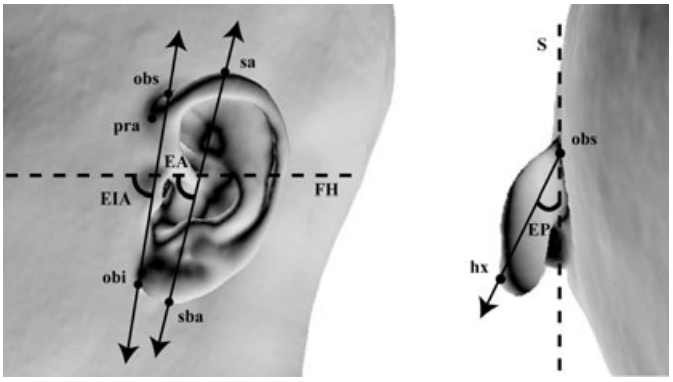

FIG. 2—*Ear angles that were measured in this study. See Tables 3 and 5 for definitions (FH = Frankfurt Horizontal; S = Sagittal plane).*

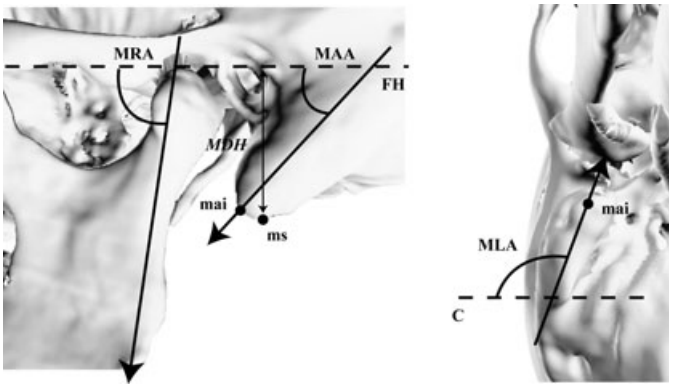

FIG. 3—*Mandibular ramus and mastoid angles that were measured in this study. See Tables 4 and 5 for definitions (FH = Frankfurt Horizontal; C = Coronal plane).*

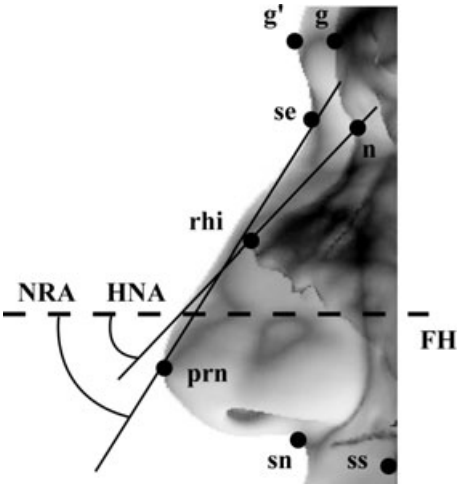

FIG. 4—*Nose angles that were measured in this study. See Tables 3, 4, and 5 for definitions (FH = Frankfurt Horizontal).*

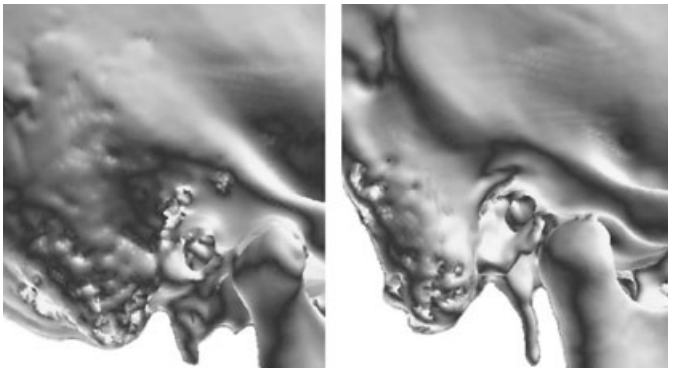

FIG. 5—*Supramastoid crest size as morphoscopically evaluated: smooth (left) and strongly developed (right).*

Furthermore, the accuracy of the previously mentioned regression equations by Heathcote (44), Asai et al. (45), and Balueva et al. (49) were examined using the CT scan data of this study and, where possible, using the aforementioned samples: (i) 3D face scan data of living subjects collected by Evison and Vorder Bruegge (n_2 = 2190, mean age = 38 years, SD = 13 years, range = 14–18 years [50]); (ii) Todd's caliper measurements of White American cadavers from the Hamann Todd Collection that were taken prior to skeletonization (n_3 = 1328, mean age = 55 years, SD = 14 years, range = 1–96 years); (iii) Todd's caliper measurements of Black American cadavers from the Hamann Todd Collection that were taken prior to skeletonization (n_4 = 1010, mean age = 41 years, SD = 16 years, range = 1–105 years); and (iv) a group of contemporary living subjects measured using manual anthropometry (n_5 = 47, mean age = 35 years, SD = 9 years, range = 22–56 years).

Ear length was calculated from Evison and Vorder Bruegge's data (50) using the "EVB_real_data.csv" file available on the '*Chapter Dataset*' CD *of Computer-Aided Forensic Facial Comparison* after individuals with missing data at landmarks 23 (superaurale) and 25 (subaurale) were removed along with any repeat measurements of the same subjects (i.e., only the first measurement counted). As Evison and Vorder Bruegge only present landmark coordinates, the Euclidean distance between sa and sba was calculated using the Pythagorean formula:

FIG. 6—*Earlobe attachment as judged morphoscopically: free (left) and attached (right).*

$$\text{Ear height} = \sqrt{(xa - xb)^2 + (ya - yb)^2 + (za - zb)^2}$$

In the formula, "*x*," "*y*," & "*z*" equal the 3D coordinates, "*a*" = landmark 23 (sa), and "*b*" = landmark 25 (sba). Note that this measurement may be slightly different from the ear length measurement taken on the CT scan subjects as Evison and Vorder Bruegge do not stipulate that their subjects were positioned in the Frankfurt Horizontal at the time of measurement. In addition, the distances calculated from the 3D coordinate data are not necessarily parallel to the median plane, as they are for the CT data.

With regard to T. W. Todd's unpublished data, the original measurements ($n = 2368$) were screened for outliers and missing values. Subsequently, 30 individuals were removed to yield two data sets: one for American Whites ($n_3 = 1328$) and one for American Blacks ($n_4 = 1010$). Young individuals (i.e., 1–18 years of age) were retained in the data sets because (i) ears at birth are close to adult size, that is, represent 75% of their values at skeletal maturity (56); (ii) linear trends in ear enlargement exist from 10 years of age (56); and (iii) a good spread of young ages was represented in these data sets, hence very young individuals did not represent outliers. Except for being taken manually using sliding calipers, these data are comparable to the CT scan measurements as they were taken following Martin's Beobachtungsblätter, with the head in the Frankfurt Horizontal (see, e.g., [35]).

Standard errors of the estimate were calculated from residuals of the predicted values obtained from the regression equations using the following equation:

$$\text{SEE} = \sqrt{\frac{\sum (a - b)^2}{n - 2}}$$

where "*a*" is the true value, "*b*" is the predicted value, and "*n*" represents the sample size.

New prediction formulae were generated using stepwise linear regression. To help evaluate the value of the regression formulae, residuals from these equations were compared with those obtained from mean measurements obtained from the CT-derived means using residual plots, SEE (described above), and the r^2. In addition, cross-validation was employed using the multiple independent samples described above. To provide comprehensive tests of Balueva et al.'s equations (49), the mean of the in-sample CT scan soft tissue depth at menton (equivalent of Balueva et al.'s gnathion [49]) was calculated and substituted for Balueva et al.'s value of 6 mm (Table 2).

As the CT sample size bordered on the smaller side for stepwise multiple regression using two independent variables ($n = 80$; see [57]), the performance of these regression equations was in addition cross-checked against their improper (unit-weighted) counterparts after recommendations by Cohen et al. (58). These improper regression models were calculated from regression on the standardized values (58–60), where +1 was substituted for positive beta weights and −1 was substituted for negative beta weights. This form of regression holds the advantage that large standard errors of the beta weights, which may be encountered in small samples, are avoided (58,59).

Data comparisons were also made against other studies to evaluate consistency of metrics, such as for ear length. Statistical calculations were undertaken using STATISTICA® (v. 7.1; Statsoft®, Tulsa, OK), SPSS® (v. 11.0; IBM®, Somers, NY), and Microsoft® Excel® (2007; Microsoft®, Redmond, WA).

TABLE 5—*Measurements taken in this study.*

Name	Abbreviation	Locality	Zone	Definition
Ear height	sa-sba	Bilateral	ST	Distance from superaurale to subaurale
Ear width	pra-pa	Bilateral	ST	Distance from preaurale to postaurale
Ear insertion height	obs-obi	Bilateral	ST	Distance from otobasion superius to otobasion inferius
Ear angle	EA	Bilateral	ST	Angle between the main axis of the ear in a lateral view and the FH
Ear insertion angle	EIA	Bilateral	ST	Angle between the axis of the ear insertion (otobasions) in a lateral view and the FH
Ear protrusion	EP	Bilateral	ST	Angle between the main axis of the ear in a superior view and the sagittal plane
Nasal dorsum length	se-prn	Midline	ST	Distance from sellion to pronasale
Nasal root angle	NRA	Midline	ST	Angle between a line formed by the sellion and the pronasale, and the FH
Soft nose height 1	se-sn	Midline	ST	Distance from sellion to subnasale
Soft nose height 2	g'-sn	Midline	ST	Distance from soft glabella to subnasale
Mastoid height	MDH	Bilateral	HT	Height of the mastoid from the mastoidale and an orthogonally projected point on the FH
Mastoid anterior angle	MAA	Bilateral	HT	Angle between the main axis of the mastoid process in a lateral view and the FH
Mastoid lateral angle	MLA	Bilateral	HT	Angle between the main axis of the mastoid process in an inferior view and the coronal plane
Mandible ramus angle	MRA	Bilateral	HT	Angle between the main axis of the posterior part of the mandibular ascending ramus and the FH
Hard nose angle	HNA	Midline	HT	Angle between a line formed by the nasion and the rhinion, and the FH
Hard nose height 1	n-ss	Midline	HT	Distance from nasion to subspinale
Hard nose height 2	g-ss	Midline	HT	Distance from glabella to subspinale
Facial height	FHN	Midline	HT	Distance from nasion to menton

ST, soft tissue; HT, hard tissue; FH, Frankfurt Horizontal; FHN, facial height of the skull.

TABLE 6—*Descriptive statistics, correlations with age, and statistical significance tests for asymmetry and sexual dimorphism.*

						Asymmetry (p-Value)			Sex						
Measurement	n	Mean	Min	Max	SD	M & F	M	F	Mean M	Mean F	SD M	SD F	t	p	Age (r)
Angles (degrees)															
MAA [R]	78	63.6	30.7	85.2	12.0	**<0.01**	0.05	**0.03**	62.1	65.4	12.3	11.5	−1.21	0.23	−0.19
MAA [L]	78	60.2	29.9	84.5	10.4				59.1	61.6	11.0	9.6	−1.05	0.29	0.01
MLA [R]	78	109.6	79.7	130.7	9.7	**0.01**	**<0.01**	0.68	107.4	112.4	9.8	8.9	−2.34	**0.03**	−0.03
MLA [L]	78	112.8	85.2	140.1	11.0				113.7	111.7	11.8	9.9	0.81	0.42	0.12
MRA [R]	78	85.8	72.8	90.0	3.9	0.73	0.83	0.43	85.4	86.3	4.0	3.7	−1.03	0.23	0.00
MRA [L]	78	85.7	73.2	90.0	4.4				85.4	86.0	4.5	4.3	−0.52	0.38	0.00
EP [R]	78	48.5	17.5	74.6	11.8	0.76	0.85	0.56	47.4	49.7	10.9	12.9	−0.85	0.40	**0.33**
EP [L]	78	48.8	20.0	89.0	11.4				47.2	50.7	10.9	11.8	−1.37	0.17	0.21
EA [R]	78	77.2	59.6	89.6	6.3	**<0.01**	0.33	**<0.01**	76.9	77.6	6.1	6.6	−0.47	0.64	0.02
EA [L]	78	75.7	60.7	89.3	6.1				76.0	75.2	6.5	5.8	0.59	0.55	0.19
EIA [R]	78	81.0	68.2	95.0	5.9	0.71	0.84	0.75	80.7	81.3	5.6	6.2	−0.42	0.68	**0.41**
EIA [L]	78	81.3	69.8	97.6	6.0				80.9	81.7	5.7	6.4	−0.58	0.56	**0.40**
NRA	77	58.2	48.6	72.5	3.9	–	–	–	58.3	58.1	4.2	3.7	0.18	0.86	0.08
HNA	77	53.3	32.5	75.2	7.0	–	–	–	52.6	54.2	7.1	6.8	−1.05	0.30	0.13
MDH [R]	78	30.0	20.2	38.0	4.1	**0.04**	0.36	**0.04**	31.8	27.7	3.3	3.9	4.96	**<0.01**	0.02
MDH [L]	78	29.5	18.7	40.5	4.0				31.5	27.1	3.2	3.4	5.87	**<0.01**	0.00
Linear distances (mm)															
se-prn	72	48.6	37.2	58.7	4.9	–	–	–	50.2	46.6	4.7	4.5	3.32	**0.01**	0.10
se-sn	71	54.7	44.9	66.7	4.8	–	–	–	56.1	53.1	4.5	4.7	2.64	**0.01**	0.05
g'-sn	73	67.1	56.5	79.1	4.6	–	–	–	68.0	66.2	4.6	4.5	1.67	0.10	0.11
n-ss	77	56.1	48.8	65.8	3.4	–	–	–	57.6	54.4	3.4	2.6	4.59	**<0.01**	−0.06
g-ss	77	66.4	59.8	75.7	3.7	–	–	–	66.7	65.9	3.7	3.7	0.97	0.33	−0.14
obs-obi [R]	78	54.8	41.7	69.7	5.5	0.27	0.90	0.09	57.2	51.7	5.6	3.6	5.05	**<0.01**	**0.58**
obs-obi [L]	78	55.1	44.1	71.2	5.5				57.2	52.4	6.1	3.2	4.19	**<0.01**	**0.62**
sa-sba [R]	78	61.7	49.5	74.3	4.9	0.34	0.31	0.84	63.8	59.0	4.8	3.7	4.92	**<0.01**	**0.47**
sa-sba [L]	78	61.9	48.2	80.1	5.6				64.3	59.1	5.5	4.3	4.52	**<0.01**	**0.50**
pra-pa [R]	78	36.6	29.7	43.9	3.2	0.40	0.33	0.73	37.9	34.9	2.8	2.9	4.67	**<0.01**	**0.33**
pra-pa [L]	78	37.0	30.9	45.3	3.6				38.5	35.2	3.2	3.3	4.58	**<0.01**	**0.32**
FHN	62	116.9	97.2	133.2	8.5	–	–	–	120.9	111.4	7.2	6.9	5.21	**0.04**	−0.02

[R], right; [L], left; M, males; F, females.
Bold type = statistically significant at $p < 0.05$.

Results

Shapiro–Wilk's test indicated that all metric measurements of the CT scans (Table 5) followed normal distributions ($p < 0.05$), except for the mandible angle. Wilcoxon test, Mann–Whitney U-test, and Spearman correlations were, therefore, used where this measurement was considered. All other variables were subject to parametric statistics.

Table 6 presents the descriptive statistics of the measurements from the CT scans, statistical significance test results, and correlations concerning asymmetry, sexual dimorphism, and age. Of note, a large and statistically significant difference existed between males and females for ear length and width (male mean, left side = 64.3 mm, SD = 5.5, $n = 43$; female mean, left side = 59.1 mm, SD = 4.3 mm, $n = 35$; $p < 0.01$). Age was also positively correlated with these ear dimensions (left side, sexes combined, $r = 0.50$ and 0.32, respectively; see also Fig. 7), but variability in measurements between individuals was large (one standard deviation represented *c.* 10% of the total ear length measurement). From this point forward, only the data for the left side of the face will be addressed.

The CT ear length measurements corresponded closely to those calculated from Evison and Vorder Bruegge's data (50), Todd's measurements on American Blacks, and the measurements on contemporary living subjects (compare to Table 7). The mean CT ear lengths were, however, *c.* 5 mm less than those calculated from the Todd data for U.S. White cadavers (Table 7).

In regards to the eight previously published ear prediction rules that were examined in this study, the following results were observed using the CT scan data:

Rule (i): The posterior jaw line (MRA) was not parallel to the orientation of the ear (EA) and these two variables were not correlated (Table 8).

Rule (ii): The height of the nose (se-sn) underestimated the ear height (sa-sba) and the height from g' to sn overestimated the height of the ear by 5.5 mm (Table 6). Positive correlations existed between the height of the nose and the ear; however, they were weak ($r = 0.30$; Table 8).

Rule (iii): The addition of a further 2 mm to the g'-sn measurement, as Gerasimov recommended, produced additional error in comparison to his recommendations tested at rule (ii).

Rule (iv): The medio-lateral orientation of the mastoid process (MLA) did not correlate with the size and orientation of the outer ear; however, there was a small correlation between the MDH and the breadth of the ear ($r = 0.41$; Table 9).

Rule (v): The breadth of the ear (pra-pa) was not equal to half its length; however, length and width were correlated ($r = 0.60$). The mean ratio of the breadth of the ear to its height was 0.59, a number which compares favorably to that reported in other contemporary studies: for example, 0.60–0.61 (39), 0.59–0.62 (41), 0.55–0.57 (43), 0.56–0.58 (34), and 0.56–0.57 (36).

Rule (vi): Development of the supramastoid crest was not related to the upper protrusion of the ear (EP); however, the protrusion of the crest is significantly linked to the ear height (sa-sba and obs-obi) and

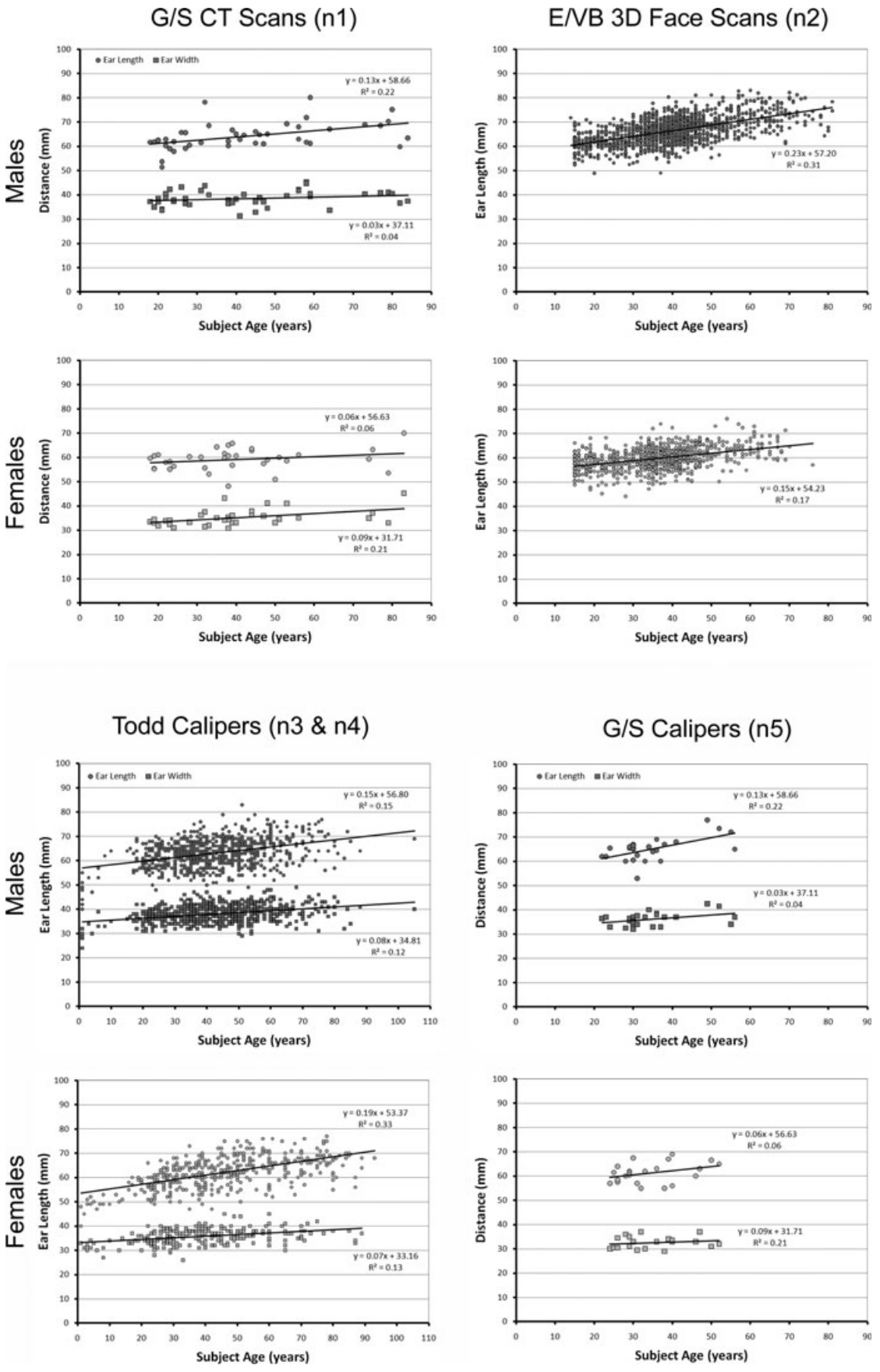

FIG. 7—*Scatterplots of the ear length and width (left side) with age.*

TABLE 7—*Sex-specific mean ear dimensions in the four samples evaluated in this study.*

						Ear Length					Ear Width				
Investigator	Measurement Method	Sex	Population	Age (Years)	*n*	Mean	SD	Min	Max	*r* (age)	Mean	SD	Min	Max	*r* (age)
Evison and Vorder Bruegge (50)	3D Face Scanner	Males	Mostly U.K.	14–81	1401	66.4	5.3	49.0	83.1	0.6	–	–	–	–	–
Todd	Anthropometry		American Whites	1–96	1160	69.4	5.8	40.0	91.0	0.4	39.0	3.5	23.0	51.0	0.2
Todd	Anthropometry		American Blacks	1–105	758	62.9	5.7	40.0	83.0	0.4	38.0	3.4	24.0	49.0	0.4
This study	Anthropometry		Mixed	24–52	22	65.1	4.9	53.0	77.0	0.6	36.1	2.7	32.0	42.5	0.3
Evison and Vorder Bruegge (50)	3D Face Scanner	Females	Mostly U.K.	15–76	789	59.8	4.5	44.2	76.1	0.4	–	–	–	–	–
Todd	Anthropometry		American Whites	1–93	168	64.4	6.1	40.0	77.0	0.5	36.0	3.8	24.0	47.0	0.4
Todd	Anthropometry		American Blacks	1–89	252	60.4	5.9	45.0	75.0	0.5	35.8	3.1	26.0	45.0	0.4
This study	Anthropometry		Mixed	22–56	25	61.3	4.1	55.0	69.0	0.3	32.5	2.4	29.0	37.0	0.2

TABLE 8—*Ear axis and ear length relationships with ramus axis and nose length measurements (*t*-tests and Pearson's correlations).*

a	b	Mean a	Mean b	SD a	SD b	*t*	*p*	*r*
EA	MRA	75.7	85.7	6.1	4.4	−11.71	<0.01	0.12
sa-sba	se-sn	61.9	54.7	5.6	4.8	8.34	<0.01	0.25
sa-sba	n-ss	61.9	56.1	5.6	3.4	7.76	<0.01	0.29
sa-sba	g-ss	61.9	66.4	5.6	3.7	−5.76	<0.01	0.01

TABLE 9—*Correlation matrix (Pearson's* r*) between the mastoid process and the outer ear.*

	EP [L]	sa-sba [L]	pra-pa [L]
MLA [L]	−0.06	0.04	−0.07
MDH [L]	−0.12	0.26	0.41

[L], left side.

orientation at its insertion (EIA). That is, individuals with protruded supramastoid crests had on average larger sa-sba, obs-obi, and EIA measurements (Table 10). In this study's sample, a strongly developed supramastoid crest was observed in 33 participants (42%) and a smooth supramastoid crest was observed in the other 45 subjects (58%). In general, no right/left asymmetry was noted.

Rule (vii): The lobe morphology (free or attached) was not related to the mastoid form or other ear measurements (Table 11). Free lobes were observed in 55 individuals (71%) and the other 23 subjects (29%) had attached lobes. No overarching right/left asymmetry was observed.

Rule (viii): The main axis of the ear (EA) was not parallel to the angle of the soft (NRA) or hard nose (HNA), and the ear and nose orientation did not correlate (Table 12). The mean difference between the ear and soft tissue nose angle in this study was 18°—slightly higher than that of other studies (33,34,47,48)—and probably as a result of defining the soft tissue nose angle from sellion to pronasale as opposed to directly running along the nasal dorsum as in other studies. The difference between the ear angulation and the angle of the hard tissue bridge of the nose was larger than the difference between the ear angulation and the angle of the soft tissue nose (mean = 23°).

TABLE 10—*Relationship between the protrusion of the supramastoid crest and the outer ear.*

	Supramastoid Crest Protrusion				
	Protruded (*n* = 33)		Smooth (*n* = 45)		
	Mean	SD	Mean	SD	*t*-Test (*p*)
EP [L]	45.9	11.1	50.9	11.2	0.05
EA [L]	74.3	6.3	76.7	5.8	0.08
EIA [L]	80.7	5.2	81.7	6.6	0.47
obs-obi [L]	57.2	6.0	53.5	4.6	**<0.01**
sa-sba [L]	64.0	6.1	60.4	4.8	**<0.01**
pra-pa [L]	38.0	3.3	36.3	3.7	**0.03**

[L], left side.
Bold type = statistically significant at $p < 0.05$.

A cross-table analysis of the supramastoid crest and the lobe morphology (Table 13) also indicated a statistically significant relationship between the crest protrusion and the lobe morphology (Pearson's $\chi^2 < 0.05$). When the crest is protruded, the lobe tends to be free. However, the inverse is not true: the attached lobe is not linked with a smooth supramastoid crest. A similar analysis showed no difference between males and females for the lobe attachment ($p = 0.87$, contingency coefficient = 0.01), but a strong relationship was detected between sex and supramastoid crest protrusion ($p < 0.01$, contingency coefficient = 0.46). In all, 86% of the females had a smooth crest versus 65% of the males.

In this sample, the orientation of the ear (EP and EA) did not correlate with the mastoid process or the bony regions of the nose (see results of matrix correlation, Table 14). The MDH correlated with the ear breadth (pra-ba), and the height of the piriform aperture (n-ss) only weakly correlated with the ear dimensions (sa-sba, pra-pa).

On the basis of the relationships between ear dimensions and sex, age, and facial height of the skull (FHN) (see above and the example scatter plots provided in Fig. 7), 12 new prediction equations were generated using stepwise regression (Table 2). In all cases, sex was transformed to a dichotomous dummy variable before entering the regression analysis (females = 0, and males = 1). Because mean soft tissue depths at menton in the CT sample differed by ≤3.5 mm from Balueva et al.'s (49) recommendation of 6 mm males = 9.5 mm, $n = 36$; females = 8.1 mm, $n = 26$), revised versions of the Balueva et al. equations using actual soft tissue depth values found in the sample were not pursued further (3.5 mm * 0.073 = 0.3 mm error).

Of the 18 regression equations evaluated in total in this study, those that disregarded sex and concerned only age produced the highest SEE (Tables 2 and 15). The ear length equation generated from Evison and Vorder Bruegge's data (no. 7) performed well on the CT scan data, but SEE was slightly lower when the equation generated from the CT scan data of this study (no. 12) was applied to Evison and Vorder Bruegge's data set. Equation no. 7 performed better than equation no. 12 on the U.S. White cadaver data and that derived from caliper measurements, but equation no. 7 performed much worse on

TABLE 11—*Relationship between the earlobe morphology and the ear/mastoid features.*

	Lobe Morphology				
	Attached (n = 23)		Free (n = 55)		
	Mean	SD	Mean	SD	t-Test (p)
MAA [L]	60.4	11.0	60.1	10.2	0.90
MLA [L]	113.9	9.6	112.4	11.6	0.59
MDH [L]	29.7	4.6	29.5	3.7	0.85
EP [L]	48.9	12.7	48.7	11.0	0.96
EA [L]	77.6	6.8	74.9	5.7	0.08
EIA [L]	82.5	7.1	80.8	5.5	0.26
obs-obi [L]	54.5	6.1	55.3	5.3	0.53
sa-sba [L]	61.8	5.5	62.0	5.8	0.86
pra-pa [L]	37.1	3.6	37.0	3.7	0.96

[L], left side.

TABLE 12—*Relationships between the ear orientation and the angle of the nose* (t-*test and Pearson's correlations).*

a	b	Mean a	Mean b	SD a	SD b	t	p	r
EA [L]	NRA	75.7	58.2	6.1	3.9	21.13	<0.01	0.02
EA [L]	HNA	75.7	53.3	6.1	7.0	21.22	<0.01	0.08

[L], left side.

TABLE 13—*Cross-table analysis of the supramastoid crest protrusion and the earlobe morphology.*

	Supramastoid Crest Protrusion	
	Developed	Smooth
Lobe	n (%)	n (%)
Attached	5 (15)	18 (40)
Free	28 (85)	27 (60)
Total	33 (100)	45 (100)

the U.S. Black cadaver sample (Table 15). Ear length equations derived on the cadaver samples (no. 8 and 10) performed well on other samples, but generally had higher SEE on the in- and out-of-sample groups than equation no. 7 or 12 (Table 15).

Ear length prediction equations of Balueva et al. (no. 5 and 6) produced similar SEE on the CT scan data as other equations reported above, but r^2 values were extremely low (<0.08; Table 15). In addition, the in-sample CT scan data indicated that FHN correlated less strongly with ear length, than did age (r^2 = 0.37 and 0.48, respectively), and regression equations based on sex and FHN (SEE = 5.1, r^2 = 0.22) performed worse than that based on both sex and age (SEE = 4.7, r^2 = 0.33; Table 2). Although r^2 values increased, with decreasing SEE, for FHN regression equations that included age (Table 2; compare equations no. 16 and 12), overfitting is possible because the ratio between sample size and the number of independent variables is further reduced (from 40–1 to 26–1, see [57–59]). For these reasons, and more importantly because mandible position must be estimated in edentulous skulls yielding additional error, any of the regression equations that include FHN as an independent variable are not recommended.

The unit-weighted regression equation for ear length (no. 13) did not perform more accurately than the proper regression equation (no. 12), even in contrast to cross-validated results, and therefore will not be further discussed here. Sex-specific mean ear lengths, derived from the CT scans, generally predicted ear length

TABLE 14—*Correlation matrix (Pearson's* r*) between the outer ear and the bony features of the ear and nose.*

	EP [L]	EA [L]	sa-sba [L]	pra-pa [L]	obi-obs [L]
MAA [L]	0.07	0.12	−0.01	−0.02	0.00
MLA [L]	−0.06	0.17	0.05	−0.07	0.03
MRA [L]	0.23	0.15	−0.09	−0.12	0.06
HNA	0.19	0.08	−0.02	−0.03	−0.01
MDH [L]	−0.13	−0.01	0.23	**0.40**	0.10
n-ss	0.01	0.13	**0.31**	**0.36**	0.14
g-ss	0.18	0.04	0.07	0.12	−0.01

[L], left side.
Bold type = statistically significant at $p < 0.05$.

TABLE 15—*Regression equation performances on different samples.*

					Out-of-Sample Data													
					G/S CT Scans Living France			E/VB 3D Face Scans Living White British			Todd Calipers Cadavers U.S. White			Todd Calipers Cadavers U.S. Black			G/S Calipers Living Mixed		
		In-Sample Data																	
Ear Dimension	Equation No. (see Table 2)	SEE	r^2	n	SEE	r^2	n_1	SEE	r^2	n_2	SEE	r^2	n_3	SEE	r^2	n_4	SEE	r^2	n_5
Length	1	UR	UR	206	6.4	0.15	78	5.2	0.25	2190	5.8	0.13	1328	6.0	0.19	1010	4.4	0.21	47
	2	UR	0.09	400	7.5	0.15	78	6.0	0.25	2190	5.7	0.13	1328	7.2	0.19	1010	5.4	0.21	47
	5	UR	UR	UR	5.4	0.08	36	–	–	–	–	–	–	–	–	–	–	–	–
	6	UR	U	UR	5.0	0.00	26	–	–	–	–	–	–	–	–	–	–	–	–
	7	4.3	0.47	2190	5.6	0.31	78	–	–	–	6.2	0.21	1328	8.0	0.20	1010	4.2	0.32	47
	8	5.4	0.21	1328	5.6	0.32	78	4.5	0.48	2190	–	–	–	–	–	–	4.1	0.31	47
	10	5.2	0.21	1328	5.0	0.25	78	5.0	0.42	2190	–	–	–	–	–	–	4.5	0.35	47
	12	4.7	0.33	78	–	–	–	5.1	0.45	2190	6.8	0.20	1328	5.4	0.16	1010	4.8	0.27	47
	13	6.9	0.33	78	–	–	–	5.6	0.46	2190	6.9	0.20	1328	6.3	0.18	1010	6.7	0.30	47
Width	9	3.5	0.11	1010	3.1	0.33	78	–	–	–	–	–	–	–	–	–	3.3	0.40	47
	11	3.1	0.19	1010	4.2	0.25	78	–	–	–	–	–	–	–	–	–	2.7	0.36	47
	14	3.1	0.29	78	–	–	–	–	–	–	3.4	0.11	1328	3.2	0.17	1010	3.2	0.40	47

E/VB, Evison and Vorder Bruegge (50); G/S, Guyomarc'h and Stephan (this study); UR, unreported; CT, computed tomography; SEE, standard errors of the estimate.

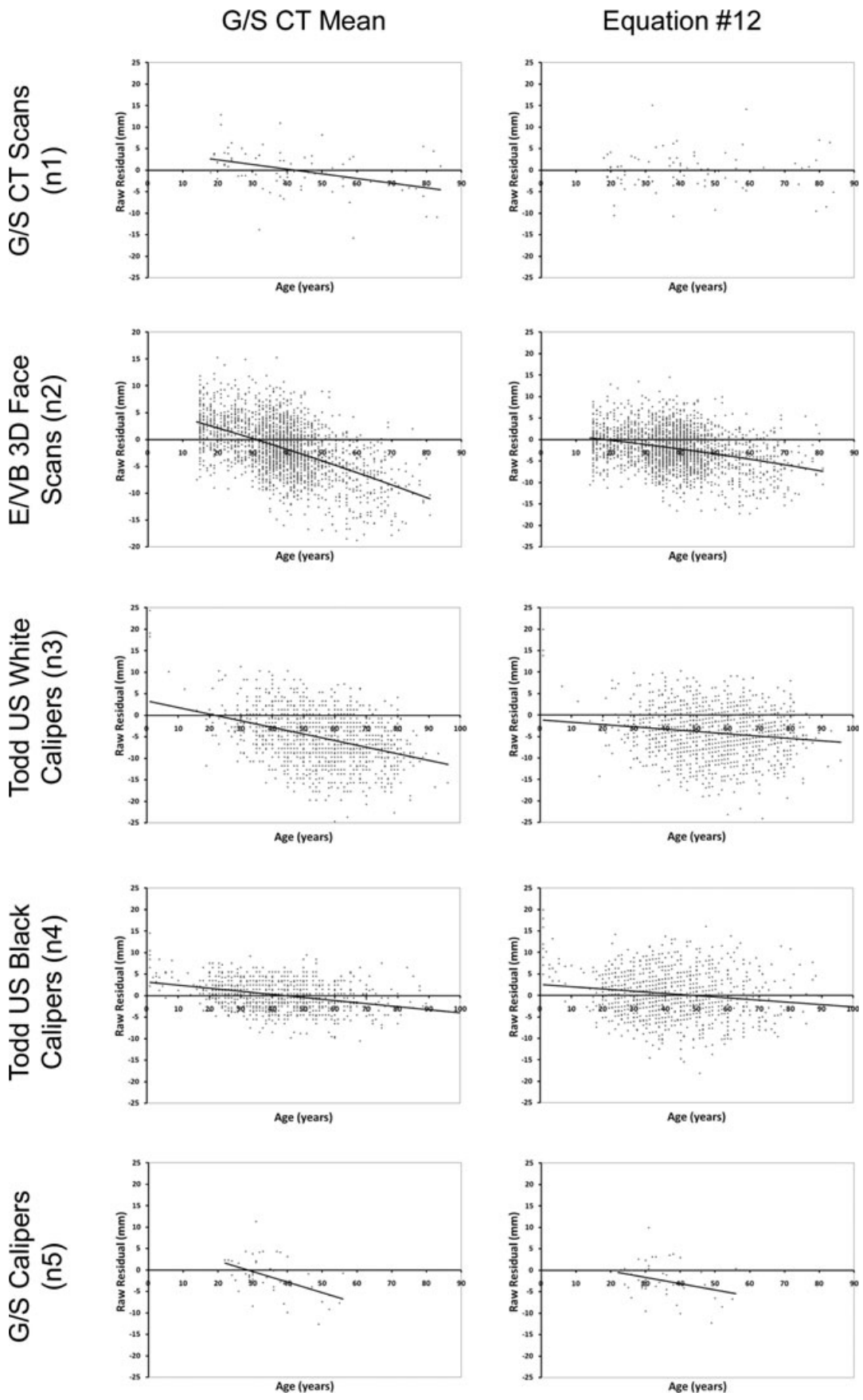

FIG. 8—*Residual plots of estimated ear lengths, by age, using the G/S computed tomography (CT) mean and equation no. 12. The slopes represent linear trend lines. For equation no. 12 in the G/S CT sample, this trend line falls on precisely on the* x*-axis.*

well (Fig. 8); however, regression equation no. 12 (and no. 7) did much better at predicting those individuals at the extremes of the age ranges (2–10 mm less error; Fig. 8). It should be noted, however, that this equation generally tended to underestimate true ear length values across the out-of-sample groups, except for extremely young individuals, whose ear length was overestimated (see Fig. 8). A regression equation for ear length using all the raw data examined in this study is presented in Table 2 (equation no. 18, $n = 4653$), but unfortunately cross-validation is not possible owing to a lack of independent data for tests. Nevertheless, robust results are expected, given the large sample size upon which this equation is derived.

With regard to ear width, the CT scan-derived equation (no. 14) performed almost as well on Todd's data and the caliper measured contemporary sample as the in-sample formulae (Table 15). However, residuals between predicted and actual ear width values indicated no value of the CT-derived regression equation above the arithmetic mean as a predictor (Fig. 9). Consequently, mean ear widths are recommended for ear width prediction above the regression equations.

Discussion

Tests of previously published face prediction rules have been conducted for many of the major facial regions (eyes, nose, and mouth), except for the ear. This study fills that gap and its results are consistent with a general pattern observed in other studies that traditionally recommended face prediction rules are not well supported by the scientific data (10–18,61).

The inaccuracies of previously published soft tissue prediction guidelines are not ambiguous or limited to few specific facial regions. Similar findings have been found on numerous occasions and often by independent teams of investigators, see, for example, results on eyeball position (13–15,61,62). In this context, the poor performance of overarching face prediction methods (see, e.g., [26,63–65]) is not surprising and mandates improvements to facilitate accurate face prediction.

This study makes some progress toward achieving this goal with specific regard to the ear. First, faces of non-Asian individuals should be constructed with free earlobes because (i) valid skeletal indicators for attached earlobes do not currently exist; (ii) supramastoid crests are associated with free earlobes (Table 13); and (iii) free earlobes tend to be more common in non-Asian groups (Tables 13 and 16). Second, orientations of the ear should follow quantified published means, either of this study (Table 6) or those published elsewhere (see, e.g., [33,34,47,48]). Third, ear length should be predicted using the proper regression equation derived from CT scans in this study (no. 12) because, so far as the data currently suggest, it provides the greatest generality that has been verified by cross-validation (Table 15 and Fig. 8). Fourth, for ear width prediction, the mean ear width should be used as it provides a simple and accurate estimator whose performance is not surpassed by the regression equations so far examined (Fig. 9). At this stage, all other characteristics of the ear can be derived from the skull only by speculation.

Although the tested guidelines presented in this study will assist facial approximation, they should not be interpreted to mean that prediction of the ear is an accurate endeavor. The magnitude of errors associated with the aforementioned four tested ear prediction guidelines is large and, in conjunction with the paucity of tested methods for ear prediction in general, underscores the inexact nature of the ear prediction process. Error in age prediction from the skeleton will also inflate errors associated with ear length prediction using the aforementioned regression equation. These inaccuracies,

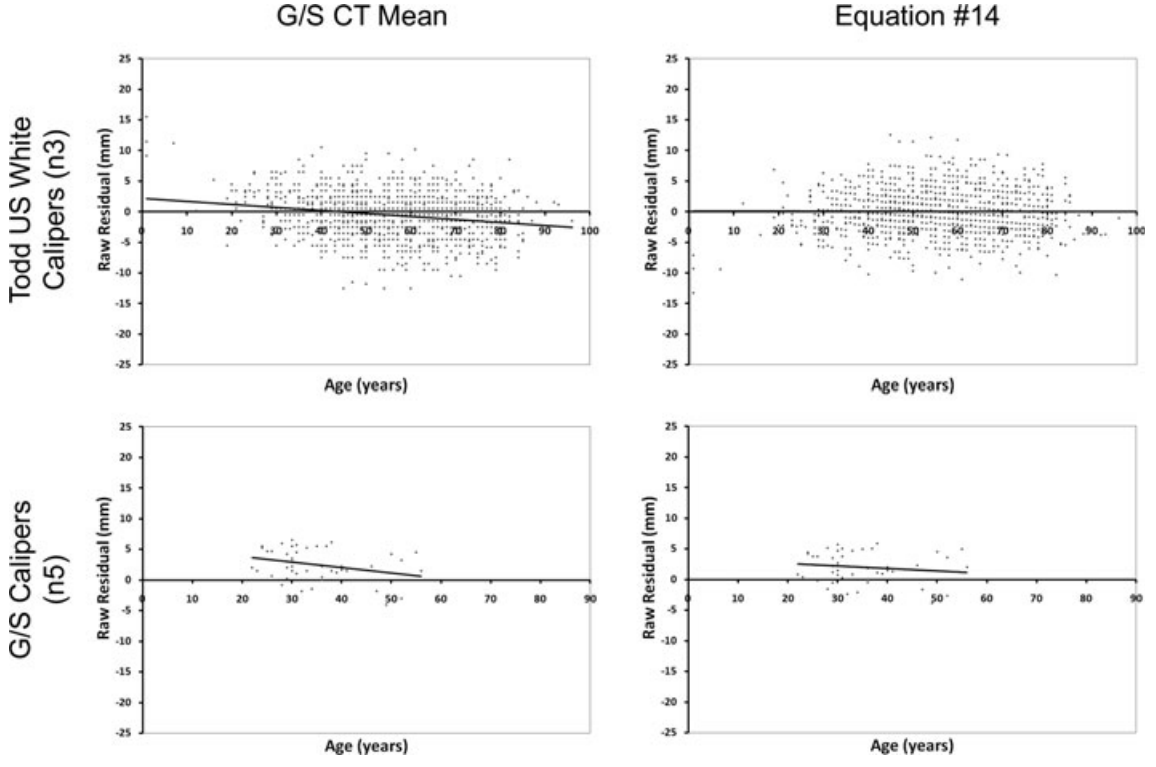

FIG. 9—*Residual plots of estimated ear widths, by age, using the G/S computed tomography (CT) mean and equation no. 14. The slopes represent linear trend lines.*

errors, and gaps in knowledge unambiguously highlight the approximate nature of the face prediction process and the sense to abandoning the term "facial reconstruction" in favor of "facial approximation."

The limited interrelationships and physical connection between the soft tissues of the ear and the temporal bone, as measured in this study, will likely hamper future attempts to improve ear prediction guidelines. Nevertheless, the large amount of variance unexplained by sex and age justifies future searches for variables that offer improvements. Moreover, landmark- and outline-based morphometric studies should be considered, as should ear relationships to other more-distant parts of the skull.

Acknowledgments

We thank Bruno Dutailly (UMR 5199 PACEA) for TIVMI assistance and the healthcare professionals who contributed to the CT scans acquisition: Pr. Christophe Aubé and Dr. Jean-Yves Tanguy (CHU Angers); Pr. Christophe Cognard, Serge Martinez, and Corinne Viard (Hôpital Purpan, Toulouse); Dr. Paul Ardilouze, Dr. David Higué, and Dr. Charles Laurent (CHCB, Bayonne); Dr. Jack Richecoeur (CH René Dubos, Pontoise); Dr. Raphaël Legghe (Polyclinique du Bois, Lille); Pr. Jean-Nicolas Dacher and Dr. Emmanuel Gerardin (CHU Rouen); Dr. Anne-Sophie Ricard and Pr. Vincent Dousset (CHU Pellegrin Tripode, Bordeaux); Pr. Michel Montaudon (Hôpital Haut-Lévêque, Pessac); Dr. Jean-Paul Delhaye (CH Pierre Ourdot, Bourgoin-Jallieu). We also thank those individuals/organizations who made raw ear data of other samples available to us for this study, in particular, (i) Evison and Vorder Bruegge for making their 3D landmark data freely and publically available for forensic facial identification research and (ii) the Cleveland Museum of Natural History, Ohio, and Lyman Jemella for T.W. Todd's original and unpublished cadaver measurements. We also thank Dr. John Byrd for critical comments on an earlier

TABLE 16—*Morphotype frequencies of the earlobe in the human population (%).*

Population	Attached	Free	Intermediate	Sample	Subjects	*n*	Study
Caucasoids	29	71	–	French	Unrelated	78	This study
	35	65	–	Indians (Indian subcontinent)	Not specified	111	(67)
	14	64	22	Indians (Indian subcontinent)	Not specified	97	(68)
	17	56	27	Indians (Indian subcontinent)	Not specified	103	(68)
	13	50	37	Indians (Indian subcontinent)	Not specified	54	(68)
	26	52	22	Indians (Indian subcontinent)	Not specified	54	(68)
	25	49	25	Indians (Indian subcontinent)	Not specified	102	(68)
	24*	77	–	Indians (Indian subcontinent)	Unrelated	107	(69)
	31	69	–	Indians (Indian subcontinent)	Unrelated	80	(69)
	23	34	43	Indians (Indian subcontinent)	Not specified	1288	(70)
	16	50	35	Indians (Indian subcontinent)	Not specified	210	(70)
	24	76	–	Indians (Indian subcontinent)	Not Specified	100	(71)
	34	66	–	Indians (Indian subcontinent)	Not Specified	119	(72)
	25	75	–	Indians (Indian subcontinent)	Not Specified	183	(72)
	41	59	–	North Americans	Not specified	380	Glass et al. (1952) cited in (69)
	25	75	–	North Americans	Not specified	241	Glass et al. (1952) cited in (69)
	84	16	–	North Americans	Families	248	(73)
	18	54	28	North Americans	Not specified	381	(74)
	16	84	–	North Brazilians	Not specified	–	Saldanha (66) cited in (69)
	23	77	–	Scottish	Not specified	500	(75)
	35	65	–	Swedish	Families	247	(76)
	33	67	–	Yugoslavs	Families	–	Berberovic and Hadziselimovic (1972) cited in (77)
Negroids	25	75	–	Nigerian	Unrelated	1600	(77)
	32	48	32	North Americans	Not specified	242	(74)
Mongoloids	62	38	–	Ahom	Unrelated	100	(78)
	29	71	–	Ahom	Not specified	330	Das (1975) cited in (78)
	64	36	–	Chinese	Not specified	79	(67)
	75†	25	–	Fijians	Not Specified	813	(46)
	65	35	–	Filipino	Not specified	49	(67)
	46	54	–	Garo	Not specified	200	Das (1967) cited in (78)
	67	33	–	Japanese	Not specified	70	(67)
	34	66	–	Kachari	Not specified	100	Das (1967) cited in (78)
	23	77	–	Kalita	Not specified	120	Das (1964) cited in (78)
	49*	51	–	Newars	Not Specified	169	(80)
	45	18	37	Nicobar Islands—Car	Not specified	341	(68)
	55	14	31	Nicobar Islands—Chowrite	Not specified	111	(68)
	27	37	37	Nicobar Islands—Terressan	Not specified	146	(68)
	65	10	25	Nicobar Islands—Southern	Not specified	119	(68)
	64	36	–	Papua New Guinean	Families	399	(67)
	23	77	–	Rabha	Not specified	300	Das (1967) cited in (78)
	26	74	–	Rajbansi	Not specified	100	Das (1967) cited in (78)
	63	37	–	Sema Naga	Not specified	100	Phukan and Begum (1976) cited in (78)
	21	79	–	Suri	Not specified	100	Das and Deka (1960) cited in (78)
	57	22	20	Tibetan	Not specified	250	(79)
Australoids	22	78	–	Australian Aborigines	Not specified	41	(67)
	50	18	32	Onge	Not specified	80	(81)

*Includes 5/6% reported as "lobe-less" in the original study.
†Includes 10% reported as "soldered" in the original study.

draft of this manuscript that inspired us to undertake cross-validation using independent samples.

References

1. Rathbun TA. Personal identification: facial reproductions. In: Rathbun T, Buikstra J, editors. Human identification: case studies in forensic anthropology. Springfield, IL: Charles C Thomas, 1984;347–62.
2. Prag J, Neave R. Making faces: using forensic and archaeological evidence. London, UK: British Museum Press, 1997.
3. Vanezis P, Blowes RW, Linney AD, Tan AC, Richards R, Neave R. Application of 3-D computer graphics for facial reconstruction and comparison with sculpting techniques. Forensic Sci Int 1989;42(1):69–84.
4. Taylor KT. Forensic art and illustration. Boca Raton, FL: CRC Press, 2001.
5. Wilkinson C. Forensic facial reconstruction. Cambridge, UK: Cambridge University Press, 2004.
6. Gibson L. Forensic art essentials. Burlington, MA: Elsevier, 2008.
7. Rogers SL. Personal identification from human remains. Springfield, IL: Charles C Thomas, 1987.
8. Tyrrell AJ, Evison MP, Chamberlain AT, Green MA. Forensic three-dimensional facial reconstruction: historical review and contemporary developments. J Forensic Sci 1997;42(4):653–61.
9. Gerasimov MM. *Vosstanovlenie lica po cerepu*. Moskva: Izdat. Akademii Nauk SSSR, 1955.
10. Stephan CN. Facial approximation: an evaluation of mouth width determination. Am J Phys Anthropol 2003;121(1):48–57.
11. Wilkinson CM, Motwani M, Chiang E. The relationship between the soft tissues and the skeletal detail of the mouth. J Forensic Sci 2003;48(4):728–32.
12. Stephan CN, Davidson PL. The placement of the human eyeball and canthi in craniofacial identification. J Forensic Sci 2008;53(3):612–9.
13. Stephan CN, Huang AJR, Davidson PL. Further evidence on the anatomical placement of the human eyeball for facial approximation and craniofacial superimposition. J Forensic Sci 2009;54(2):267–9.
14. Stephan CN. Facial approximation: falsification of globe projection guideline by exophthalmometry literature. J Forensic Sci 2002;47(4):1–6.
15. Guyomarc'h P, Dutailly B, Couture C, Coqueugniot H. Anatomical placement of the human eyeball in the orbit—validation using CT scans of living adults and prediction for facial approximation. J Forensic Sci 2012;e-pub ahead of print. DOI:10.1111/j.1556-4029.2012.02075.x.
16. Stephan CN, Henneberg M, Sampson W. Predicting nose projection and pronasale position in facial approximation: a test of published methods and proposal of new guidelines. Am J Phys Anthropol 2003;122(3):240–50.
17. Rynn C, Wilkinson CM. Appraisal of traditional and recently proposed relationships between the hard and soft dimensions of the nose in profile. Am J Phys Anthropol 2006;130(3):364–73.
18. Stephan CN, Devine M. The superficial temporal fat pad and its ramifications for temporalis muscle construction in facial approximation. Forensic Sci Int 2009;191(1):70–9.
19. Rynn C, Wilkinson CM, Peters HL. Prediction of nasal morphology from the skull. Forensic Sci Med Pathol 2010;6(1):20–34.
20. Stephan CN, Henneberg M. Predicting mouth width from inter-canine width—a 75% rule. J Forensic Sci 2003;48(4):725–7.
21. Guyomarc'h P, Coqueugniot H, Dutailly B, Couture C. Predictability and facial approximation: a 3D geometric morphometric investigation of the nasal morphology. In: Buhl CA, Engel F, Hartung L, Kästner M, Rüdell A, Weisshaar C, editors. Proceedings of the 4th Meeting of Junior Scientists in Anthropology; 2010 March 25–28; Freiburg, Germany. Freiburg, Germany: Universität Freiburg, 2010;84–97.
22. Haig ND. The effect of feature displacement on face recognition. Perception 1984;13(5):505–12.
23. Haig ND. Exploring recognition with interchanged facial features. Perception 1986;15(3):235–47.
24. Welcker H. *Schiller's schadel und todtenmaske, nebst mittheilungen uber schadel und todtenmaske kant's*. Braunschweig: Viehweg F and Son, 1883.
25. Montagu A. Location of porion in the living. Am J Phys Anthropol 1939;25(2):281–95.
26. Eggeling Hv. *Die Leistungsfahigkeit physiognomischer rekonstruktionsversuche auf grundlage des schadels*. Archiv Anthropol 1913;12:44–7.
27. Broadbent TR, Mathews VL. Artistic relationships in surface anatomy of the face: application to reconstructive surgery. Plast Reconstr Surg 1957;20(1):1–17.
28. Jordanov J. Head reconstruction by the skull. Sofia, Bulgaria: Marin Drinov Academic Publishing House, 2003.
29. Ullrich H, Stephan CN. On Gerasimov's plastic facial reconstruction technique: new insights to facilitate repeatability. J Forensic Sci 2011;56(2):470–4.
30. Gatliff BP. Facial sculpture on the skull for identification. Am J Forensic Med Pathol 1984;5(4):327–32.
31. Krogman WM, Iscan MY. The human skeleton in forensic medicine, 2nd edn. Springfield, IL: Charles C Thomas, 1986.
32. Fedosyutkin BA, Nainys JV. The relationship of skull morphology to facial features. In: Iscan MY, Helmer RP, editors. Forensic analysis of the skull. New York, NY: Wiley-Liss, 1993;199–213.
33. Farkas LG, Hreczko TA, Kolar JC, Munro IR. Vertical and horizontal proportions of the face in young adult North American Caucasians: revision of neoclassical canons. Plast Reconstr Surg 1985;75(3):328–37.
34. Farkas LG, Hreczko TM, Katic M. Craniofacial norms in North American Caucasians from birth (one year) to young adulthood. In: Farkas LG, editor. Anthropometry of the head and face. New York, NY: Raven Press, 1994;241–336.
35. Martin R. *Lehrbuch der anthroplogie*. Jena, Germany: Gustav Fischer, 1928.
36. Farkas LG, Ngim RCK, Lee ST. Craniofacial norms in 6-, 12-, and 18-year-old Chinese subjects. In: Farkas LG, editor. Anthropometry of the head and face. New York, NY: Raven Press, 1994;337–46.
37. Bozkir MG, Karakas P, Yavuz M, Dere F. Morphometry of the external ear in our adult population. Aesthetic Plast Surg 2006;30(1):81–5.
38. Brucker MJ, Patel J, Sullivan PK. A morphometric study of the external *ear: age- and sex-related differences*. *Plast Reconstr Surg* 2003; 112(2):647–52.
39. Ferrario VF, Sforza C, Ciusa V, Serrao G, Tartaglia G. Morphometry of the normal human ear: a cross-sectional study from adolescence to mid-adulthood. J Craniofac Genet Dev Biol 1999;19(4):226–33.
40. Meijerman L, van der Lugt C, Maat GJR. Cross-sectional anthropometric study of the external ear. J Forensic Sci 2007;52(2):286–93.
41. Sforza C, Grandi G, Binelli M, Tommasi DG, Rosati R, Ferrario VF. Age- and sex-related changes in the normal human ear. Forensic Sci Int 2009;187(1–3):110.e1–7.
42. Alexander M, Laubach LL. Anthropometry of the human ear (a photogrammetric study of USAF flight personnel): Areospace Medical Research Laboratories; Aerospace Medical Division; Air Force Systems Command; Wright-Patterson Air Force Base, Ohio, 1968;Report No.: AMRL-TR-67-203.
43. Purkait R, Singh P. Anthropometry of the normal human auricle: a study of adult Indian men. Aesthetic Plast Surg 2007;31(4):372–9.
44. Heathcote JA. Why do old men have big ears? Br Med J 1995;311(7021):1668.
45. Asai Y, Yoshimura M, Nago N, Yamada T. Correlation of ear length with age in Japan. Br Med J 1996;312(7030):582.
46. Gabel NE. A racial study of the Fijians. Anthropol Rec 1958;20(1):11–22.
47. Skiles MS, Randall P. The aesthetics of ear placement: an experimental study. Plast Reconstr Surg 1983;72(2):133–40.
48. Farkas LG. Discussion—the aesthetics of ear placement: an experimental study. Plast Reconstr Surg 1983;72(2):139–40.
49. Balueva TS, Veselovskaya EV, Rasskazova AV. A comparison of the medieval and modern populations of the Novgorod region, based on *facial reconstruction*. *Archaeol Ethnol Anthropol Eurasia* 2010;38(3): 135–44.
50. Evison MP, Vorder Bruegge RW, editors. Computer-aided forensic facial comparison. Boca Raton, FL: CRC Press, 2010.
51. Spoor CF, Zonneveld FW, Macho GA. Linear measurements of cortical bone and dental enamel by computed tomography: applications and problems. Am J Phys Anthropol 1993;91(4):469–84.
52. Guyomarc'h P, Santos F, Dutailly B, Desbarats P, Bou C, Coqueugniot H. Three-dimensional computer-assisted craniometrics: a comparison of the uncertainty in measurement induced by surface reconstruction performed by two computer programs. Forensic Sci Int 2012;e-pub ahead of print. DOI: 10.1016/j.forsciint.2012.01.008.
53. Farkas LG. Anthropometry of the head and face. New York, NY: Raven, 1994.
54. Bräuer G. Osteometrie. In: Knussmann RMR, editor. *Anthropologie handbuch der vergleichenden biologie des menschen*. Stuttgart, Germany: Fisher, 1988;160–231.
55. Krogman WM, Sassouni V. Syllabus in roentgenographic cephalometry. Philadelphia, PA: College Offset, 1957.

56. Niemitz C, Nibbrig M, Sacher V. Human ears grow throughout the entire lifetime according to complicated and sexually dimorphic patterns—conclusions from a cross-sectional analysis. Anthropol Anz 2007;65(4):391–413.
57. Tabachnick BG, Fidell LS. Using multivariate statistics, 5th edn. New York, NY: Pearson Education, 2007.
58. Cohen J, Cohen P, West SG, Aiken LS. Applied multiple regression/correlation analysis for the behavioral sciences, 3rd edn. Mahwah, NJ: Lawrence Eribaum Associates, 2003.
59. Cohen J. Things I have learned (so far). Am Psychol 1990;45(12):1304–12.
60. Dawes RM. The robust beauty of improper linear models in decision making. Am Psychol 1979;34(7):571–82.
61. Detorakis ET, Drakonaki E, Papadaki E, Pallikaris IG, Tsilimbaris MK. Effective orbital volume and eyeball position: an MRI study. Orbit 2010;29(5):244–9.
62. Wilkinson CM, Mautner SA. Measurement of eyeball protrusion and its application in facial reconstruction. J Forensic Sci 2003;48(1):12–6.
63. Stephan CN, Henneberg M. Building faces from dry skulls: are they recognized above chance rates? J Forensic Sci 2001;46(3):432–40.
64. Quatrehomme G, Balaguer T, Staccini P, Alunni-Perret V. Assessment of the accuracy of three-dimensional manual craniofacial reconstruction: a series of 25 controlled cases. Int J Legal Med 2007;121(6):469–75.
65. Mackenzie D. Putting a face to a skull. New Sci 2006;2554(19):26–7.
66. Saldanha PH. Frequencies of consanguineous marriages in north east of Sao Paulo, Brazil. Acta Genet Stat Med 1960;10:71–88.
67. Lai LYC, Walsh RJ. Observations on earlobe types. Acta Genet Stat Med 1966;16(3):250–7.
68. Dutta PC, Ganguly P. Further observations on earlobe attachment. Acta Genet Stat Med 1965;15:77–86.
69. Chattopadhyay PK. A note on the earlobe attachment among the Jats and Ahirs. Acta Genet Stat Med 1968;18(3):277–82.
70. Basu A. Observations on earlobe attachments in some population groups of Mysore (India). Acta Genet Stat Med 1968;18(4):380–5.
71. Dutta PC. A note on the earlobe. Acta Genet Stat Med 1963;13:290–4.
72. Basu A. A note on the earlobe. Acta Genet Stat Med 1966;16:184–5.
73. Wiener AS. Complications in ear genetics. J Hered 1937;28(12):425–6.
74. Dronamraju KR. Earlobe attachment in the Buffalo region. Acta Genet Stat Med 1966;16(3):258–64.
75. Riddel WJB. Studies in the classification of eye colour. Ann Eugen 1942;2:266–73.
76. Hildén K. *Über die form des ohrläppchens beim menschen und ihre abbägigkeit von erbanlagen*. Hereditas 1922;3:351–7.
77. Williams GO, Hughes AE. Frequencies of attached and free earlobes in Lagos (Nigeria). Am J Phys Anthropol 1987;72(3):399–401.
78. Dutta MN. Earlobe attachment among the ahom of Dibrugarh, Upper Assam. Curr Anthropol 1979;20(2):399.
79. Tiwari SC, Bhasin MK. Frequency of hand clasping and earlobe attachment in Tibetans. Hum Hered 1969;19(6):658–61.
80. Bhasin MK. Earlobe attachment among Newars of Nepal. Hum Hered 1969;19(5):506–8.
81. Pal A. Earlobe attachment of the Onge. Hum Hered 1970;20(6):650–3.

Additional information and reprint requests:
Pierre Guyomarc'h, Ph.D.
Joint POW/MIA Accounting Command
Central Identification Laboratory
310 Worchester Avenue, Building 45
Joint Base Pearl Harbor-Hickam, HI 96853-5530
E-mail: Pierre.Guyomarch.FRN@jpac.pacom.mil